Biosensors and Bioelectronics 25 (2010) 1859–1868

Contents lists available at ScienceDirect

Biosensors and Bioelectronics

journal homepage: www.elsevier.com/locate/bios

Review

Nanomaterial-assisted aptamers for optical sensing

Guoqing Wang[a], Yunqing Wang[a], Lingxin Chen[a,*], Jaebum Choo[b,**]

[a] Yantai Institute of Coastal Zone Research, Chinese Academy of Sciences, Yantai 264003, China
[b] Department of Bionano Engineering , Hanyang University, Ansan 426-791, South Korea

ARTICLE INFO

Article history:
Received 7 September 2009
Received in revised form 28 October 2009
Accepted 11 November 2009
Available online 17 November 2009

Keywords:
Aptamer
Nanomaterial
Aptamer sensor
Optical sensing

ABSTRACT

Aptamers are single-strand DNA or RNA selected *in vitro* that bind specifically with a broad range of targets from metal ions, organic molecules, to proteins, cells and microorganisms. As an emerging class of recognition elements, aptamers offer remarkable convenience in the design and modification of their structures, which has motivated them to generate a great variety of aptamer sensors (aptasensors) that exhibit high sensitivity as well as specificity. On the other hand, the development of nanoscience and nanotechnology has generated nanomaterials with novel properties compared with their counterparts in macroscale. By integrating their strengths of both fields, recently, versatile aptamers coupling with novel nanomaterials for designing nanomaterial-assisted aptasensors (NAAs) make the combinations universal strategies for sensitive optical sensing. NAAs have been considered as an excellent sensing platform and found wide applications in analytical community. In this review, we summarize recent advances in the development of various optical NAAs, employing various detection techniques including colorimetry, fluorometry, surface-enhanced Raman scattering (SERS), magnetic resonance imaging (MRI) and surface plasmon resonance (SPR).

Contents

1. Introduction

Aptamers are short single-strand DNAs (ssDNAs)/RNAs that bind diverse targets beyond DNAs or RNAs with high affinity and specificity, which are normally screened with a combinatorial

* Corresponding author. Tel.: +86 535 2109130; fax: +86 535 2109000.
** Co-corresponding author. Tel: +82 31 400 5201; fax: +82 31 436 8188.
E-mail addresses: lxchen@yic.ac.cn, chenlxcn@yahoo.com (L. Chen), jbchoo@hanyang.ac.kr (J. Choo).

0956-5663/$ – see front matter © 2009 Elsevier B.V. All rights reserved.
doi:10.1016/j.bios.2009.11.012

technique called systematic evolution of ligands by exponential enrichment (SELEX). In the process of SELEX, more than 10^{10} number of random sequences of nucleic acids in the initial libraries are subjected to a selection pressure, resulting in an exposure of sequences with binding properties. The ssDNAs/RNAs binding to the target are then eluted from the mixture. After polymerase chain reaction (PCR) amplification, the products are subjected to the next round of selection. The selection cycles continue until the final high-affinity ssDNA/RNA species for the target are identified. It is believed that nucleic acids not only play crucial roles in biological processes, but also are versatile tools for target recognition in analytical community. Since discovery in 1990s (Tuerk and Gold, 1990; Ellington and Szostak, 1990), many aptamers have been selected for corresponding targets including metal ions, organic molecules, biomolecules, and even microorganisms/cells, relying on their special three-dimensional (3D) structures. When aptamers bind their targets, they may either incorporate small molecules into their nucleic acid structures or be integrated into the structures of macromolecules (Hermann and Patel, 2000). In comparison with their equivalents of antibodies, aptamers possess several advantages for construction of biosensors such as cost-effective synthesis, high binding affinities for their targets (Brody et al., 1999) and flexibility for signal transduction and detection (Liu et al., 2009). Moreover, aptamers are superior to antibodies in bioanalysis owing to the lack of immunogenicity (Nimjee et al., 2005) and stability against biodegradation and denaturation (Liu and Lu, 2006). Finally, it is easy to design diverse ultra-selective probes for specific targets based on the well-known secondary structures of aptamers with minimum knowledge of their tertiary structures (Liu and Lu, 2004, 2007a).

It is well-known that a sensor consists of at least two elements, namely, target recognition and signal transduction. Once high-specificity aptamers are attained, the next advancement in aptamer sensors (aptasensors) would be employment of novel strategies for sensitive biosensing. Nanomaterials have recently emerged as ideal candidates enabling efficient signal transduction and amplification in aptasensors. The nanomaterial-assisted aptasensors (NAAs) display unprecedented advantages in sensing applications and have attracted significant interests of multidisciplinary study. Since several previous reviews have covered principles and applications of aptasensors (Hamula et al., 2006; Song et al., 2008; Liu et al., 2009; Nguyen et al., 2009), we herein focused on the design and working performance of optical NAAs where the optical detections are adopted for aptasensor signal harvesting. These optical NAAs can be analyzed in-depth as followings:

The NAAs are sensing platform with high selectivity and sensitivity. Generally, aptamers change their conformation after binding with targets. By taking advantage of the conformation change, it allows designing reasonable sensing platforms with assistance of nanomaterials. The selectivity of a sensing approach is achieved by capitalizing on the binding affinity and specificity of aptamer to its target, while the sensitivity is dependent on the capacity of nanomaterials to transduce the binding event to detectable signal.

The optical NAAs are to transduce aptamer recognition events to physically measurable signals. Optical detection methods such as colorimetry, fluorescence, surface-enhanced Raman scattering (SERS) and surface plasmon resonance (SPR) are most widely adopted for signal harvesting in aptasensors because of their ease of use and high sensitivity. Also, fluorescence, SERS and magnetic resonance imaging (MRI), are suitable for *in vivo* sensing, showing great potential for practical applications. Nanomaterials in NAAs usually magnify the transduced originally weak signals by several orders of magnitude in aptasensors, which make the optical NAAs highly sensitive.

In this review, for good understanding of optical NAAs, the highlights and prominent examples were summarized, based on various detection methods such as colorimetry, fluorometry, SERS, MRI and SPR. The latest advances and prospects in the development of NAAs were also discussed.

2. Approaches to bioconjugate aptamers with nanomaterials

In NAAs, aptamers and nanomaterials usually work as labels for supporting each other, dramatically broadening the extension of biological applications. For optimization of NAAs, it is important to verify the combination methods of aptamers and nanomaterials. Nanomaterials exhibiting unique surface effect provide facile ways for interacting with aptamers. Mainly, there are two bioconjugation approaches for coupling aptamers with nanomaterials, namely covalent linkage and non-covalent linkage. Covalent linking involves a chemisorption method that is widely used. For example, thiolated-aptamers can be easily chemisorbed onto the surfaces of gold nanoparticles (AuNPs) while the amine-labeled aptamers can be easily adsorbed on the surface of carboxyl-modified silica nanoparticles (SiNPs). Non-covalent assembly involving a physical adsorption provides an alternative bioconjugation approach. Li and Rothberg (2004a,b) found that negatively charged aptamer can adsorb onto negatively charged AuNP surface based on electrostatic adsorption mechanism. This finding has assisted to create modification-free bioconjugations and opened possibility for simple, time-saving analysis procedure. Based on complementary electrostatic interactions, polyamine with positive charge in solution can act as a bridge between aptamer and nanoparticle and promote the weak surface adsorption (Graham and Faulds, 2008). Specific biomacromolecular interactions such as streptavidin/biotin complementarity have also been applied to provide aptamer–nanomaterial binding. For instance, streptavidin-coated nanomaterials would easily adsorb biotinylated aptamers onto their surface. The hybridization of aptamers and nanoparticle-tagged DNA has also been used to conduct NAAs for target detection, which is another popular format for combining aptamers with nanomaterials (Zhao et al., 2007a). The above mentioned approaches are expected to conduct integrated NAA sensing systems and to enhance the recognition efficacy and transduced signals.

3. Applications of NAAs for optical sensing

3.1. Colorimetric assay

Metallic nanoparticles possessing size-/distance-dependent optical properties are ideal candidates for colorimetric assays. For example, the color of colloidal gold is sensitive to its aggregation/dispersion due to varying interparticle plasmon coupling and resulting surface plasmon band shift. Furthermore, owing to AuNPs' extinction coefficient being over 1000 times higher than that of organic dyes (Ghosh and Pal, 2007), the AuNP-based colorimetric recognitions provide considerable sensitivity (Rex et al., 2006). Accordingly, assembly/disassembly of nanoparticles can be considered as the novel indicator of colorimetric assay. AuNP-based colorimetric sensing has been a subject of great interest over the past decade, which takes advantage of the color change that results from the interparticle plasmon coupling during AuNPs aggregation (red to purple/blue) or redispersion of AuNP aggregates (purple to red). Since invented for DNA analysis (Mirkin et al., 1996), the colorimetric assay has been expanded for the detection of a variety of targets, including proteins (Pavlov et al., 2004; Huang et al., 2005), metal ions (Liu and Lu, 2003), small organic compounds (Zhao et al., 2008) and even whole cells (Medley et al., 2008).

3.1.1. Aptamer-directed AuNP assay

Aptamer-functionalized AuNPs are mostly used for colorimetric sensing, where AuNPs act as the color indicators while aptamers act as functional targeting molecules. An early example was colorimetric protein assay using aptamer–AuNP nanoprobes for the amplified detection of thrombin (Pavlov et al., 2004), which was essential in coagulation and therapy of cardiovascular disease (Becker and Spencer, 1998). Since thrombin includes two sites for the aptamer sandwich binding, by attaching aptamers to a glass surface, functionalized AuNPs would be localized on the glass surface for colorimetric detection in the presence of thrombin. For higher sensitivity, the growth of immobilized AuNPs was followed in solution that included $HAuCl_4$ and reducing agent, concomitantly with the coupling of enlarged AuNPs and higher absorbance spectra. This optimized optical sensor achieved a detection limit of 2 nM, one order of magnitude lower than that without the latter process. Jana and Ying (2008) improved this method based on dot–blot assays. They applied aptamer-conjugated silica-coated AuNPs for recognizing thrombin immobilized on nitrocellulose membrane. The brown/red color would be observed in minutes with naked eye owing to the localization of the nanoparticles. The advantages of AuNPs with silica coating are its robust stability and enhanced optical cross-section. By depositing gold on the nanoparticle surfaces, the color changes were highly amplified and the detection limit measured by naked eye was down to 25 nM. Huang et al. (2005) developed a colorimetric method for platelet-derived growth factors (PDGFs) and platelet-derived growth factor receptor (PDGFR) based on extinction changes of AuNPs modified with PDGF aptamers. As shown in Fig. 1A, in the presence of PDGF, interparticle cross-linking of AuNPs was induced by PDGF molecules that acted as bridges linking aptamer-modified AuNPs together. However, the cross-links of AuNPs decreased in the presence of high-concentration PDGF due to repulsion and steric effects resulted from saturated AuNP surfaces. As a result, AuNPs aggregation degree underwent biphasic stages upon increasing PDGF concentration gradually. On the basis of binding competition between aptamers and PDGFR to PDGF, the PDGFR could still be detected with a detection limit of 3.2 nM.

Significantly, a direct colorimetric assay for cancer cells was developed by Tan and coworkers (Medley et al., 2008). AuNPs modified with aptamers specific for CCRF-CEM cells (CCL-119 T-cell, human acute lymphoblastic leukemia) were incubated with target cells. Relying on the selective recognition property, aptamers directed the assembly of AuNPs on the membrane surfaces of target cells as a result. The assembled AuNPs acted like a larger μm-scaled gold structure, which interacted efficiently with the light and exhibited significantly increased scattering and absorption coefficients compared to that of individual AuNP owing to the surface plasmon interaction. Thus the target cells were labeled with distinct color change while no spectra change of absorption could be observed even in complex control samples (fetal bovine serum). By measuring the absorbance changes of AuNPs in the presence of target cells and control cells, a high sensitivity of 90 cancer cells were demonstrated in addition to excellent selectivity.

3.1.2. DNA–AuNP network-based assay

Generally, previous strategies of NAAs for colorimetric assays confine the analysis only to analytes capable of supplying two more binding sites or being immobilized. Fortunately, DNA–AuNP network unveils a general methodology for colorimetric sensing, especially for the detection of environmental heavy metal ions exhibiting simplicity and high sensitivity compared with laborious inductively coupled plasma approaches. For example, a novel method for Hg^{2+} detection on the basis of T (thymidine)-Hg^{2+}-T

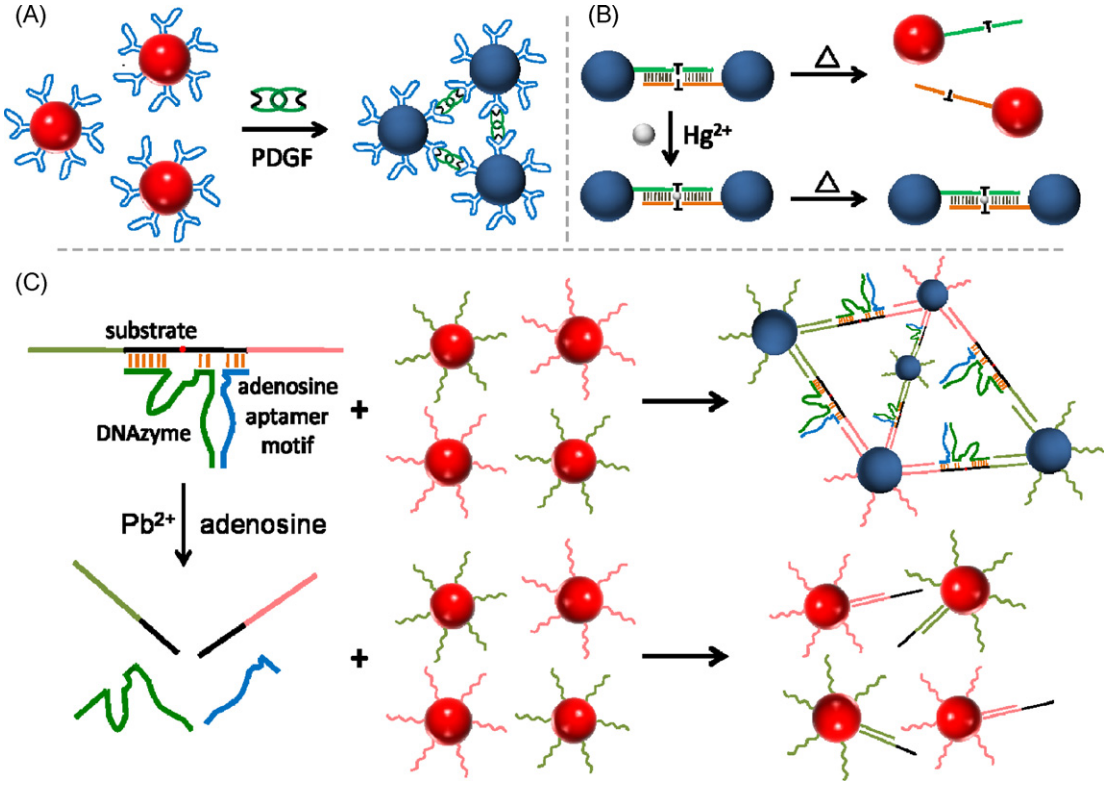

Fig. 1. Colorimetric assays based on aptamer-directed AuNP aggregation/suspension. (A) PDGF sensing using aptamer-directed assembly of AuNPs in the presence of PDGF. (B) Hg^{2+} detection relying on Hg^{2+}-induced stabilization of DNA duplex linked-AuNP aggregates. Reprinted with the permission from Liu et al. (2009). Copyright 2009 American Chemical Society. (C) Adenosine sensing based on a DNAzyme with a motif that can regulate the DNAzyme activity in the presence of adenosine. Reprinted with the permission from Liu and Lu (2004). Copyright 2004 American Chemical Society.

coordination was reported by Lee et al. (Tanaka et al., 2007; Lee et al., 2007a). AuNPs first assembled through hybridization of their surface DNA, where a T–T mispair was intentionally designed. As shown in Fig. 1B, when heated to the temperature of dissociating duplex DNA, AuNP aggregates became suspended and tinctorially red except the ones containing Hg^{2+} due to the strong linking force from Hg^{2+}-mediated T–T base pairs. The melting temperature (T_m) of DNA–AuNP networks was found to rise linearly with increasing concentration of Hg^{2+}. However, it was found that the T_m of the Hg^{2+}-stabilized DNA–AuNP networks decreased in the presence of cysteine (Lee et al., 2008a) that could bind with Hg^{2+} with high affinity and remove it from T–T mismatch sites. Among various amino acids, only cysteine brought a significant decrease of T_m. The competitive assay for cysteine was highly selective and achieved a detection limit of 100 nM. For Hg^{2+} detection at room temperature, Lee and Mirkin (2008) immobilized DNA–AuNPs in a chip for scanometric detection based on the same principle. Following with silver enhancement, the sensitivity was improved from 100 nM in the previous assay to 10 nM.

Liu and Lu (2003, 2006) developed a general sensor for target detection using aptamer/DNAzyme-linked DNA–AuNP networks. Blue AuNP aggregates for sensing adenosine consisted of two kinds of AuNPs (functionalized with either 3′ or 5′ thiolated DNA) and a linker DNA used for capturing targets, which hybridized with thiolated DNA on AuNP surfaces. Upon introducing adenosine to the network structures, the binding between adenosine and aptameric region in linker DNA was triggered so that the purple aggregates were fast disassembled to a detectable red color. This colorimetric sensor could achieve detect limits of 300 μM and 50 μM for adenosine and cocaine, respectively. DNAzymes with metal-dependent catalyst activities have been shown promising for designing metal ion biosensors. The biosensors for Pb^{2+} (Liu and Lu, 2003) and Cu^{2+} (Liu and Lu, 2007b) using metal cofactor-specific DNAzyme coupled with AuNPs have successively emerged. To expand range of analytes of DNAzyme-based biosensors, aptazymes (or allosteric DNAzymes) were designed for various targets based on the combination of aptamer and DNAzyme (Liu and Lu, 2004, 2007a). Liu and Lu (2004) reported a colorimetric adenosine sensor using aptazyme-directed assembly of AuNPs. As shown in Fig. 1C, the aptazyme relied on the Pb(II)-specific DNAzyme with an adenosine aptamer motif that can modulate the DNAzyme activity through allosteric interactions depending on the presence of adenosine. The aptazyme was inactive and the substrate strands served as linkers to assemble AuNPs, resulting in a blue color. The presence of adenosine activated the aptazyme and led to cleavage of the substrate. Disassembly of AuNP aggregates resulted in a red color. Adenosine of 100 μM could be measured with high selectivity. Therefore, aptazyme sensors can be designed regardless of whether the analytes are directly involved in the cleavage reaction or not.

3.1.3. Assay via controlling surface charge of AuNPs

AuNPs in suspension are mainly stabilized by adsorbed anions. The resulting repulsion overcomes the strong van der Waals attraction force between AuNPs and prevents them from aggregating. Accordingly, the control of surface charge on AuNP surface would be a novel approach for colorimetric detection. Normally, double strand DNA (dsDNA) possesses higher charge density than ssDNA due to the negatively charged phosphate groups along the DNA backbone. The electrostatic repulsion between AuNPs modified with dsDNA is therefore stronger than that modified with ssDNA. Based on this simple concept, Zhao et al. (2007a) presented a method for target detection via an aptamer hybridized with a short complementary oligonucleotide attached to AuNPs in a chosen salt concentration. Upon binding adenosine, the aptamers were dehybridized and released to the solution, thus weakening the electrostatic repulsion between AuNPs. As a result, AuNPs aggregated

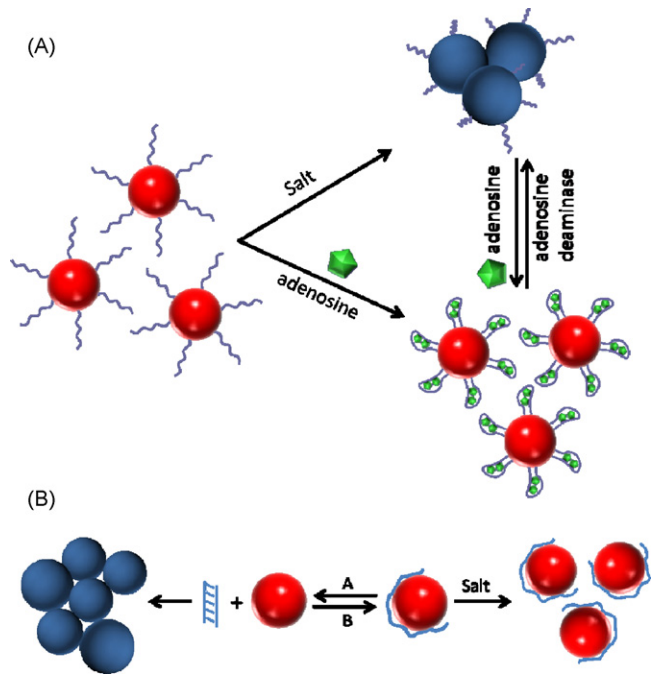

Fig. 2. (A) Stabilization of suspended AuNPs from salt-induced aggregation upon adenosine-induced aptamer folding. Reprinted with the permission from Zhao et al. (2008). Copyright 2008 American Chemical Society. (B) Label-free colorimetric assay relying on different interaction of unfolded/folded DNA with AuNPs. Binding analyte "A" induces conformational change of unfolded DNA to folded DNA while adding analyte "B" causes a contrary process.

with color change to purple that was used as the indicator of this assay, causing a detection limit of 10 μM. Surface charge density of AuNPs could also be controlled with the changes of aptamer folding/unfolding conformation on the AuNP surfaces. It was found that folded aptamer-modified AuNPs were more stable toward salt induce aggregation than those tethered to unfolded aptamers. As shown in Fig. 2A, based on this fact and the predictable structure switching of aptamer, analysis of adenosine and adenosine deaminase was successfully realized (Zhao et al., 2008).

Interestingly, the label-free colorimetric assay was developed by employing vastly different ability of unfolded DNA and folded DNA to stabilize AuNPs in the presence of salt (Li and Rothberg, 2004a,b). In other words, unfolded DNA would adsorb onto AuNP surfaces and enhance the electrostatic repulsion between AuNPs, and thus effectively stabilize AuNPs against salt-induced aggregation, while folded DNA does not possess this protective property. As seen from Fig. 2B, target-induced structure switching of aptamer leads to the aggregation/dispersion of AuNPs. Lee et al. (2008b) reported the comparison of labeled (DNA–AuNPs network-based) and label-free DNAzyme-AuNP system for colorimetric detection of UO_2^{2+}, which showed that the label-free assay was fast and simple. The excellent detection limit and linear response range were 1 nM and 1–100 nM, respectively, compared to 50 nM and 50–500 nM for the labeled system. The limit of label-free sensing system was at its lower stability than the prepared labeled colorimetric sensor.

Thus far, various strategies have been developed for colorimetric assay via versatile aptamers and AuNPs with unique properties. The major advantage of aptamer–AuNP-based colorimetric assays is that molecular recognition events can be transformed into color changes, which could be monitored by absorption spectroscopy or visual observation, thus no sophisticated instruments are required. Furthermore, because of high extinction coefficients of the nanoparticles, these assays can provide relatively high sensitivity for potential applications in rapid screening with qualitative and semi-quantitative requirements. However, colorimetric

methods are not applicable for colored samples. Also, substable nanoparticles/nanoaggregates during assembly/disassembly often induce unstable signals, which are undesirable and should be overcome for practical applications in the future.

3.2. Fluorometric assay

It has been well established that the recognition events between aptamers and targets take place with the change of aptamer conformations. Upon reasonable design, such conformational change may be applied for varying the local environment of fluorophores or nanomaterials, and therefore altering the emission properties of fluorescent systems. Compared to colorimetry, fluorescence approaches show more promising applications in measuring bio-interactions in aquatic environment because of the flexible ways in quantitative analysis with high sensitivity and wide response range (Chen et al., 2008b; Kim et al., 2007; Jung et al., 2007). Traditional organic dyes associate with the problem of narrow absorption, broad emission, photobleaching and so on, unable to meet the expectations. Recently, functional nanomaterials possessing fluorescence quenching/emission have been extensively utilized to probe dynamic biological processes using electron-transfer quenching or fluorescence resonance energy transfer (FRET) as photophysical probing mechanisms, which have opened a new way for signaling assistance in aptasensors.

3.2.1. Nanomaterial quencher-based assay

Besides high extinction coefficient for colorimetric assay, AuNPs exhibit superquenching property of fluorescence through energy/charge transfer processes. Particularly, the Stern–Volmer quenching constants of dye–AuNP pairs are usually several orders of magnitude greater than those of dye-organic quencher pairs (Fan et al., 2003). Based on this unique feature, Huang et al. (2007) demonstrated a PDGF assay using aptamer-modified AuNPs. PDGF aptamer has a unique triple-helix conformation structure with which a fluorophore of *N*,*N*-dimethyl-2,7-diazapyrenium dication (DMDAP) can be intercalated. Hence, the incubation with aptamer–AuNPs brought DMDAP close to AuNPs and thus its fluorescence was quenched. Upon PDGF binding, the conformation of aptamer changed and therefore block of the DMDAP intercalation, making the fluorescence of DMDAP strongly restored. They applied aptamer–AuNPs to capture and enrich PDGF from large-volume samples, obtaining a detection limit of 8 pM. Afterward, a new competitive homogeneous photoluminescence quenching assay of PDGF was described using photoluminescent Au nanodots (AuNDs, 2.0 nm) as donors and AuNPs as acceptors (Huang et al., 2008a). The addition of PDGF to 11-mercaptoundecanoic acid-protected AuNDs resulted in the formation of PDGF-AuND bioconjugates on the basis of electrostatic and hydrophobic interactions. By introducing aptamer-modified AuNPs, the photoluminescence was quenched by AuNPs because the high affinity between PDGF and aptamer brought the AuNDs close to AuNPs. In the presence of PDGF or PDGFR, however, the interaction between PDGF-AuNDs and aptamer-modified AuNPs decreased and the photoluminescence restored as a consequence of competitive reactions. This method was further applied to the detection of PDGFs in urine samples from healthy persons. The result (0.10 ± 0.02 nM) agreed well with reported value (0.047–0.11 nM) (Gersuk et al., 1989). Lee et al. (2009) designed a fluorescence sensor for Hg^{2+} analysis in a microarray format using polydiacetylene liposome nanoparticles (PLNs) as indicators. As a unique conjugated polymer, polydiacetylene can display pressure-sensitive tunable color and fluorescence. When Hg^{2+} was present, the resulting bulky T–Hg^{2+}–T complexes denoted strong steric repulsion between the folded aptamer strands and perturbation of the ene–yne backbone of the polydiacetylene liposomes, inducing fluorescence as well as color variation of PLNs. This PLN-based microarray implied a new and simple integrated technique for aptasensors.

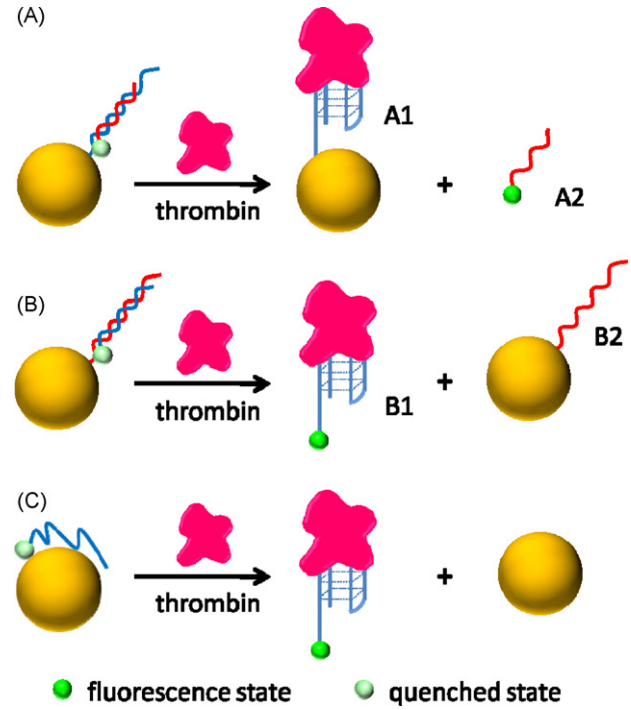

Fig. 3. Diagram of three strategies for fluorescent assay of thrombin. Reprinted with the permission from Wang et al. (2008a). Copyright 2008 Elsevier.

Wang et al. (2008a) systematically investigated three general strategies for fluorescent assay of thrombin depending on different interactions between aptamers and AuNPs. As shown in Fig. 3, these sensing principles using AuNPs as fluorescence quenchers would be separately described as followings. (A) Thiolated thrombin aptamer A1 was immobilized on AuNPs and hybridized with dye-labeled ssDNA A2. Added thrombin bound with aptamer and induced dissociation of A2 and subsequent fluorescence recovery. (B) Thiolated B2 was immobilized on AuNPs and hybridized with dye-labeled aptamer B1. The binding of thrombin led the release of aptamer B1 and fluorescence recovery. (C) Dye-labeled aptamer adsorbed on AuNPs. The addition of thrombin caused the conformation change of aptamer and the negatively charged aptamer released from AuNPs, resulting in the fluorescence recovery. Particularly, the (C) strategy was simple, fast and convenient. However, it was associated with the problem of nonspecific adsorption of aptamers on AuNPs. This led to broad distribution of both equilibrium constant and rate constant in desorption and low sensitivity of 3.5 nM. Though the (A) and (B) strategies gave more complicated procedures, the better uniformity and sensitivity could be achieved because of the homogeneous preparation and recognition. The method (A) was recommended due to its lower detection limit (0.14 nM), in comparison with method (B) (3.78 nM).

Besides AuNPs, Au nanowire (AuNW) (Huang and Chen, 2008) and carbon nanotube (CNT) have also been used as fluorescence quencher for fluorescent sensing. Yang et al. (2008) reported a CNT quenching-based fluorescent biosensor for probing thrombin. Dye-labeled thrombin aptamer assembled on CNT with π-stacking between nucleotide bases and CNT sidewalls, inducing fluorescence quenching ascribed to the electron or energy transfer from the fluorophore to the CNT. Conversely, the fluorescence signal dramatically increased in the presence of thrombin due to the aptamer-target competitive binding interaction. The assay

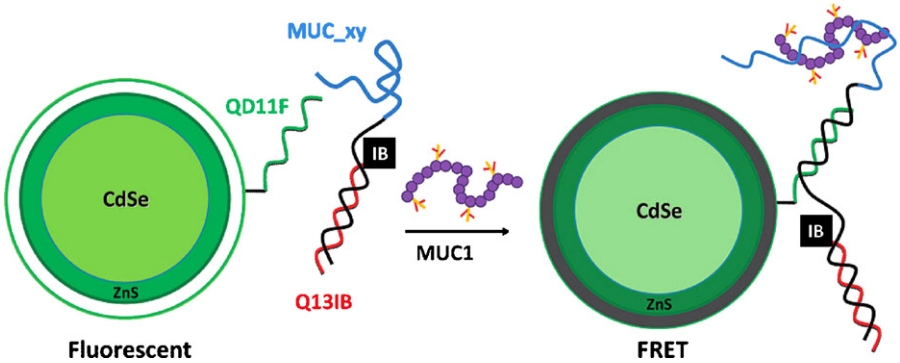

Fig. 4. Fluorescent assay of mucin 1 using target-induced fluorescence quenching based on the hybridization between QD-labeled DNA strand and quencher-labeled DNA strand.
Reprinted with the permission from Cheng et al. (2009). Copyright 2009 American Chemical Society.

achieved a detection limit of 1.8 nM with a dynamic response range of 4.0–150 nM.

3.2.2. Aptameric quantitative assay using fluorescent nanoparticle

For advantages of narrow, tunable and highly stable photoluminescence over organic fluorophores, quantum dots (QDs) combing with aptamers foreshow a class of novel fluorescent nanoprobes for biosensing applications. Choi et al. (2006) devised simple aptamer-capped PbS QDs (λ_{em} = 1050 nm) for thrombin detection. The photoluminescence of this nanostructure gradually decreased with increasing thrombin amount, which was thought to result from the selective aptamer–thrombin interaction and therefore charge transfer between thrombin functional group (e.g., amine) and QD conduction band. This fluorescence probe could detect thrombin as low as 1 nM with a linear range spanning 1–30 nM.

Cheng et al. (2009) reported an aptamer-based detection approach for mucin 1 (an epithelial tumor marker) using a 3-component DNA hybridization system with CdSe/ZnS QDs. As shown in Fig. 4, a DNA strand containing aptameric region partially pre-hybridized with an Iowa Black FQ quencher strand. After the addition of QD-labeled DNA that complementary with part of aptamer strand, strong fluorescence intensity of QD reporter was observed since QDs cannot get close to the quencher. Indeed, the aptameric region folded into its inherent secondary structure based on intramolecular Waston–Crick interaction, thus prevented the hybridization. In the presence of mucin 1, decrease in fluorescence intensity was detected since binding of mucin 1 to the aptameric region broke the intramolecular base paring and facilitated the hybridization of aptamer strand and QD-labeled strand, allowing the quencher to be brought near enough to the QDs, which induced the occurrence of FRET. A linear response can be established for approximate range found in blood serum at nM-level detection limit.

SiNPs and magnetic nanoparticles (MNPs) have also been used in fluorescent assays. A novel adenosine monophosphate (AMP) sensor was designed by Song et al. (2009) based on a MNP–aptamer–SiNP sandwich complex (Fig. 5). Rubpy dye-doped SiNPs and silica-coated MNPs were synthesized and modified with oligonucleotides as linkers. AMP aptamers were introduced to hybridize the oligonucleotides and assemble SiNPs and MNPs into sandwich hybrids. In the presence of AMP, the aptamer preferred to form stable complex with AMP and directed the disassembly of

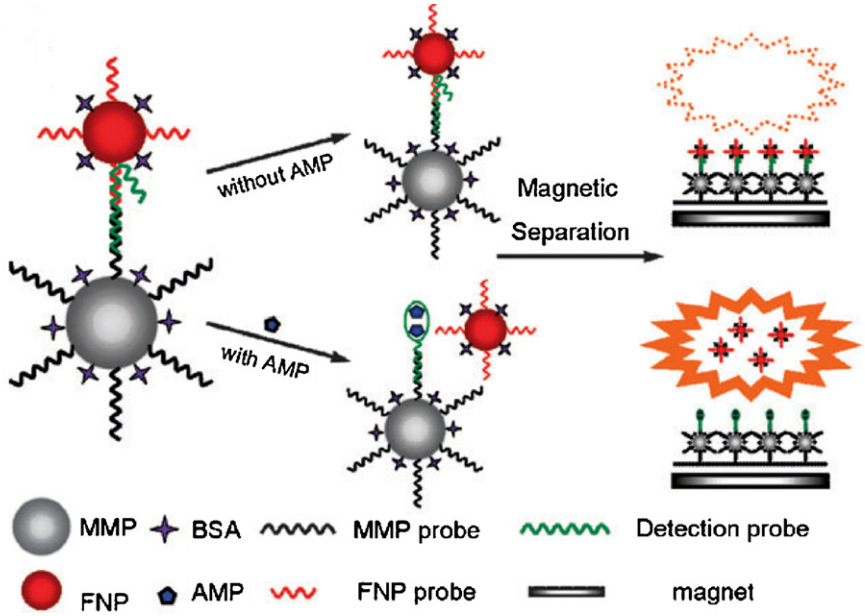

Fig. 5. Schematic presentations of SiNPs and MNPs-assisted AMP aptasensor.
Reprinted with the permission from Song et al. (2009). Copyright 2009 The Royal Society Chemistry.

sandwich hybrids. Upon magnetic separation, the fluorescence of SiNPs was detected for AMP analysis.

3.2.3. Aptamer-directed NAAs for cell targeting and therapy

Recent years have witnessed that aptamer-directed NAAs are ideal candidates for cell-surface proteins recognition and therefore cancer cell targeting. Biocompatible nanomaterials used as carrier of recognizer moieties for optical imaging offer a number of advantages such as directness of observation, improvement of targeting efficacy and feasibility of photothermal therapy. Aptamer-conjugated MNPs have been used for the collection and detection of multiple cancer cells (Smith et al., 2007). Three different leukemia cell lines, CCRF-CEM cells, Ramos cells (CRL-1596, B-cell, human Burkitt's lymphoma) and Toledo cells (CRL-2631, non-Hodgkin's B cell lymphoma) were mixed for extraction and detection tests. CEM cell-specific aptamer-conjugated MNPs were incubated with the cell mixtures. Magnetic separation and washing process were successively performed. Then, Rubpy dye-doped SiNPs modified with CEM aptamers were incubated with the extracted CCRF-CEM cells for labeling. Consequently, the detection of CCRF-CEM cells in cell mixtures could be achieved using fluorescence microscope. This aptamer-MNP conjugates have manifested benefits of efficient, fast and selective potential determinations of clinical diagnostics. Huang et al. (2008b) synthesized dye-labeled aptamer-modified Au–Ag nanorod (Au–Ag NR, 12 nm × 56 nm) for efficient CCRF-CEM cell targeting. Compared to affinity of single aptamer, that of aptamers assembled on Au–Ag NR surfaces was shown to increase by 26-fold determined by flow cytometry. The selective photothermal therapy of mixed carcinomar cells was further presented (Huang et al., 2008c), which are key challenges in cancer therapy.

QDs have gained popularity in this research domain for years since the problems associated with water solubility and biocompatibility were solved (Bruchez et al., 1998; Chan and Nie, 1998). Chen et al. (2008d) constructed a QD-labeled GBI-10 aptamer for targeting U251 cells (a human glioma cell line), on which surface tenascin-C is overexpressed as an extracellular matrix protein. The CdSe/ZnS QDs were first converted from hydrophobic to hydrophilic to produce QD-COOH for H_2N-aptamer conjugation. After probe synthesis completion, QD-labeled aptamers were incubated with target and control cells. The high fluorescence of U251 cell images was consistent with the high affinity of aptamer to tenascin-C while no fluorescence was observed on the surface of control cells. Conjugation of aptamers with QDs makes it possible to realize synchronous cancer imaging, therapy, and sensing of drug delivery. Bagalkot et al. (2007) functionalized QDs (λ_{em} = 500 nm) with aptamers that are specific for prostate-specific membrane antigen (PSMA) expressing on LNCaP cell surface, and then intercalated doxorubicin (Dox, a fluorescent anthracycline drug emitting at 520–640 nm) into the double-stranded CG sequences in PSMA aptamer. The formation of this nanostructure resulted in quenching of both QDs and Dox based on a Bi-FRET mechanism: QD fluorescence was quenched by Dox while the fluorescence of Dox was quenched by intercalation within the aptamer. After incubating the aptamer-QD-Dox conjugates with target cells, Dox was released from the conjugates, resulting in fluorescence recovery of both QDs and Dox in cells. This strategy was sensitive to detect cancer at a single cell level since both QDs and Dox gave sharp images of cancer cells with low background noise. Recently, Choi et al. (2009) have demonstrated the improved ability of aptamer-passivated nanocrystals to inhibit growth of cancer cells (MCF-7 breast cancer cells). Aptamer sequences of GT and AGRO can bind target proteins and form cytotoxic complexes while also serving as templates for PbS QDs and Fe_3O_4 nanoparticles. The aptamer-passivated nanocrystals could significantly reduce proliferation of target cells and exhibited 3–4 times enhanced growth inhibition efficacy compared to aptamers alone, unveiling a new way in clinical diagnosis.

In the above fluorescent assays, NAAs coupling with fluorescence detection show a wide variety of sensing principles relying on functional nanomaterials. Aptamers labeling with fluorophores also provide simple approaches and facilitate the real-time detection. The theoretically limitless variety of analytes offers great opportunity for fluorescent NAAs to find numerous practical applications in many aspects of analytical community.

3.3. SERS-based assay

As another well-known analytical method, SERS possesses high sensitivity, generally 6–10 orders of magnitude over conventional Raman spectroscopy. In addition, it is possible to obtain an enormous Raman enhancement using hot-spots on aggregated silver nanoclusters. The enhancement factors are estimated to be 14–15 orders, which are much larger than the ensemble-averaged values (Nie and Emory, 1997). SERS therefore provides a sensitivity that is comparable with fluorescence detection. Moreover, it has several intrinsic advantages over fluorometry such as fingerprints of analytes, excitation at any wavelength, alleviated photobleaching and narrow peak widths. Also, reproducible and quantitative SERS detections have been achieved (Lee et al., 2007b; Chen and Choo, 2008). By coupling with SERS, NAAs open up a whole new application area of biosensors.

3.3.1. Assay via controlling distance between reporter and substrate

Apparently, signal enhancements of Raman scattering can be achieved with Raman active molecules attached to SERS substrate. Raman intensity is determined by either the distance between reporter molecules and SERS substrate or adsorbate intensity on SERS substrate (Wang et al., 2009a), Based on this principle, it is possible to design SERS-based aptasensors. Wang et al. (2007a) reported the first SERS-based aptasensor for thrombin detection. Aptamers were immobilized on Au substrate to capture targets. Aptamer-modified, Rhodamine 6G (R6G)-adsorbed AuNPs were then localized on this substrate due to the binding between aptamers and the second thrombin binding sites. After depositing silver nanoparticles (AgNPs) on the AuNPs, the Raman scattering of R6G was enhanced for thrombin detection. This aptameric SERS sensor can detect thrombin as low as 0.5 nM. Cho et al. (2008) further presented a simple SERS-based sensor for thrombin detection. Raman reporter (methylene blue, MB) tethered thrombin aptamer thiolated at 5′end was adsorbed on AuNP-coated substrate. Upon introduction of the target protein, the aptamer underwent a binding-induced conformation change. The physically adsorbed aptamer was displaced from AuNP surface while the chemisorbed aptamer remained and provided a baseline signal level for the reduced signals.

Various SERS-based aptasensors have also been developed by taking advantage of target-induced conformation change of aptamers. Chen et al. (2008a) designed a cocaine aptasensor based on the principle that the addition of cocaine causes the aptamer folding into a rigid three-way junction, resulting in close proximity of Raman label (tetramethylrhodamine, TMR) to Ag colloid film and enhancement of Raman scattering. The SERS signal difference could be even distinguished with the presence of 1 μM cocaine compared to blank. In another work (Chen et al., 2008c) (Fig. 6A), anti-adenosine 32-mer aptamer was employed to hybridize with a TMR-labeled 12-mer complementary DNA. In the presence of adenosine, the dsDNA probe preferred to form a stable adenosine–aptamer complex. The released TMR-DNA was then incubated with probe DNA on a SERS substrate. This brought DNA hybridization and therefore TMR approached to SERS active surface to give a detectable signal for adenosine.

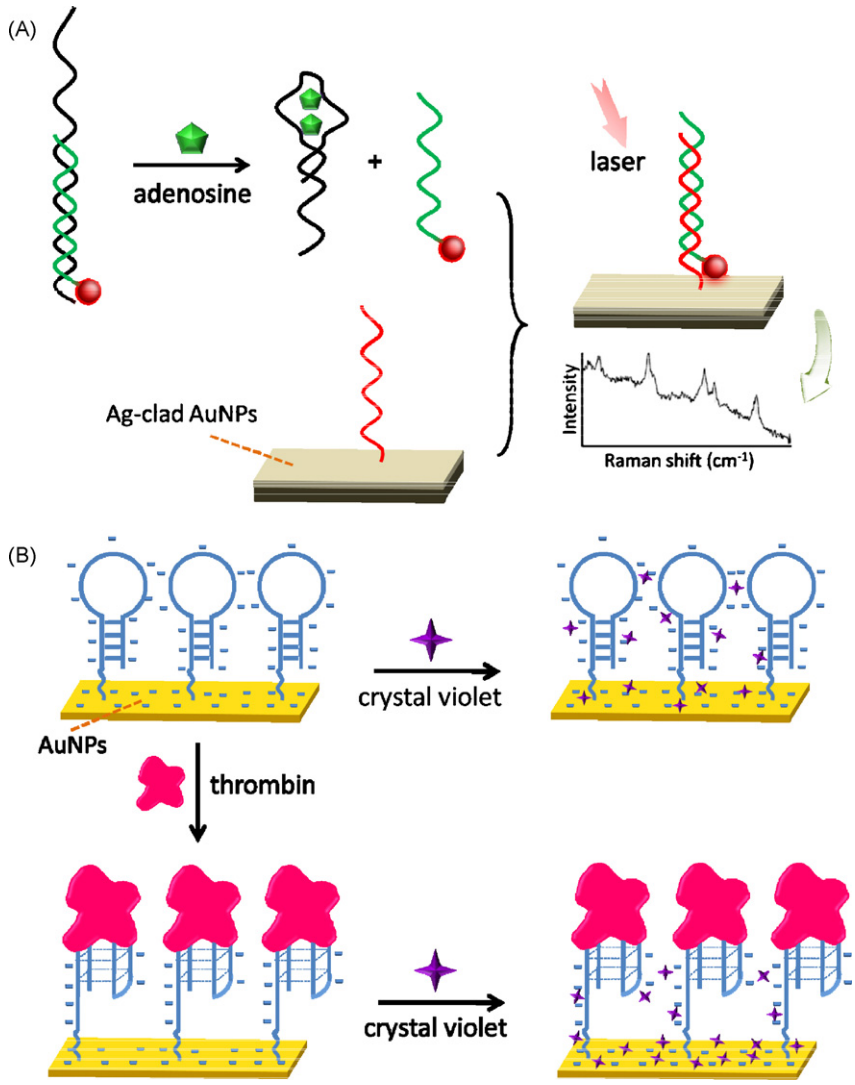

Fig. 6. (A) SERS-based adenosine detection using structure-switching aptamer. Short DNA strand released by target addition hybridizes with its probe DNA on SERS substrate and generates SERS signal. Reprinted with the permission from Chen et al. (2008c). Copyright 2008 Elsevier. (B) Thrombin detection according to the different amount of CV molecules absorbed on SERS substrate due to target-induced different electrostatic effect of the anchored aptamer. Reprinted with the permission from Hu et al. (2009). Copyright 2009 American Chemical Society.

Hu et al. (2009) described a novel thrombin assay using the change of electrostatic interaction between aptamer and crystal violet (CV) molecules (Fig. 6B). They first immobilized "hairpin"-like thrombin aptamer strands on AuNP-coated SERS substrate. The addition of CV to the functionalized substrate only gave a weak SERS signal due to the barrier effect of the aptamer. If the target was presented prior to CV addition, the binding-induced change of aptamer conformation could weaken the barrier effect of aptamer and facilitate CV adsorption on AuNPs, giving rise to strong SERS signal for thrombin. This method displayed excellent selectivity and a linear detection range of 0.1–10 nM with a detection limit of 20 pM.

3.3.2. Aggregation-based assay

It is commonly regarded that aggregated nanoparticles provide much higher Raman enhancement factor than single one. Accordingly, target-induced aggregation of nanoparticles can be conducted for novel "signal on" SERS detection. Wang and Chen (2009b) demonstrated a SERS-based assay for Hg^{2+} using aptamer-conjugated AgNPs. TAMRA-labeled Hg^{2+} aptamer linearly adsorbed on and densely covered AgNP surfaces in the presence of spermine, which is used to promote the surface adsorption of negatively charged aptamer and reduce the negative charge on AuNPs (Graham and Faulds, 2008). This resulted in the initiation of aggregation and a weak SERS signal. However, the presence of Hg^{2+} would cause the change of aptamer conformation, leading to the exposure of AgNP surfaces and reduced electrostatic repulsion. As a result, the more aggregated AgNPs formed nanoclusters with "hot-spots" that provided excellent surface enhancement of SERS signals from the reporter. This sensing system showed a detection limit of 5 nM, lower than the maximum allowable level (10 nM) in drinking water defined by U.S. Environmental Protection Agency.

NAAs coupling with SERS detection possess advantages such as relatively high sensitivity and alleviated photobleaching. Since Raman reporters have distinct and resolvable Raman fingerprints, SERS-based aptasensors have a tremendous capacity for multiplex assays. However, uniform SERS substrates and nanomaterials for homogenous and more reproducible SERS assays are still in demand.

4. Conclusions and outlook

The recent advances in the development of various optical NAAs for a wide range of targets have been reviewed, most of which utilize the detection methods of colorimetry, fluorometry

Table 1
List of diverse nanomaterials with novel optical properties in aptasensors.

Signaling methods	Nanomaterials	Functions employed	Targets
Colorimetry	AuNP	Size-dependent properties, high extinction coefficient	CCRF-CEM cells (Medley et al., 2008), thrombin (Pavlov et al., 2004), PDGF (Huang et al., 2005), cysteine (Lee et al., 2008a), ATP (Wang et al., 2007a), adenosine (Liu and Lu, 2004; Zhao et al., 2008), cocaine (Liu and Lu, 2006), Pb^{2+} (Liu and Lu, 2003), Hg^{2+} (Lee et al., 2007a), Cu^{2+} (Liu and Lu, 2007b), UO_2^{2+} (Lee et al., 2008b)
Fluorometry	AuNP	Fluorescence quenching	Thrombin (Wang et al., 2008a), PDGF (Huang et al., 2007), adenosine and cocaine (Liu et al., 2007), Hg^{2+} (Liu et al., 2008)
		Fluorescence emission	PDGF (Huang et al., 2008a)
	AuNW, CNT	Fluorescence quenching	Thrombin (Huang and Chen, 2008; Yang et al., 2008)
	MNP	Magnetic separation	CCRF-CEM, Ramos and Toledo cells (Smith et al., 2007), AMP (Song et al., 2009)
	QD	Fluorescence emission	PSMA (Chu et al., 2006; Bagalkot et al., 2007), glioma cells (Chen et al., 2008d), mucin 1 (Cheng et al., 2009), thrombin (Levy et al., 2005; Choi et al., 2006), cocaine and adenosine (Liu et al., 2007)
	SiNP	Fluorescence emission	AMP (Song et al., 2009), CCRF-CEM, Ramos and Toledo cells (Smith et al., 2007)
		Ease of separation	ATP (Wang et al., 2008b)
	Au–Ag NR	Photothermal convector	CCRF-CEM cells (Huang et al., 2008c)
	Poly(lactic acid)-block PEG copolymer nanoparticle	Encapsulating drugs for controlled release	LNCaP cells (Farokhzad et al., 2004); PSMA cells (Zhang et al., 2007)
	Chitosan nanoparticles	Fluorescence emission	CCRF-CEM cell (Tallury et al., 2009)
	PLN		Hg^{2+} (Lee et al., 2009)
SERS	AgNP, AuNP, Ag-clad AuNP	Raman enhancement	Thrombin (Wang et al., 2007b; Cho et al., 2008; Hu et al., 2009), cocaine (Chen et al., 2008a), adenosine (Chen et al., 2008c), Hg^{2+} (Wang and Chen, 2009b)
MRI	Iron oxide nanoparticle	Superparama-gnetism	Thrombin (Yigit et al., 2008), adenosine (Yigit et al., 2007)
SPR	AuNP	SPR signal enhancement	Adenosine (Wang and Zhou, 2008)
	Au-capped oxide nanostructure		Thrombin (Kim et al., 2008)
Light scattering	AuNP	High contrast degree and size-dependent optical properties	MDA-MB-231 and Hs578T cells (Huang et al., 2009)
Reflectance imaging			1483 cells and SiHa cells (Nitin et al., 2007), PSMA cell (Javier et al., 2008)

and SERS. More related works are summarized in Supplementary Information (Table S1). Other optical signal-harvesting detection methods like MRI and SPR have also been summarized in Section 3.4 (Supplementary Information). Up to now, approximately 250 aptamers have been sequenced. The recent progress in SELEX techniques enables rapid and efficient selections of aptamers for targets within only a few hours (Lou et al., 2009; Park et al., 2009) compared to traditional SELEX requiring several weeks to months. Nanomaterials with different optical, magnetic and electric properties provide powerful tools to design ideal signal-enhanced optical NAAs, which are summarized in Table 1. To meet the challenge of selectivity and sensitivity, more novel nanomaterials will be created and further employed for NAA design and application. The use of other detection techniques such as quartz crystal microbalance (QCM), surface acoustic wave (SAW) and micro-cantilevers is encouraged to provide label-free and one-step sensing.

The development of NAAs merges the field of life science, material science and chemistry. With the great progress in both aptamers and nanomaterials, optical NAAs show ideal sensing performances and promising potentials in analytical community. Meanwhile, we notice that most of the above assays were demonstrated in buffer systems as proof-of-concept. When NAAs are expected to find practical applications in analytical community, including bioanalysis, biomedical diagnosis, environmental monitoring and forensic science, the performances of NAAs need to be carefully evaluated due to the significant matrix effects in complex samples. Moreover, once a great number of NAAs are attained, the next puzzling challenge will be the integration of mature micro/nanofabrication techniques (e.g. microarrary and microfluidics) that allows the generation of ultrasensitive, portable and low-cost NAAs for more sophisticated analysis.

Acknowledgements

This work was supported by the National Natural Science Foundation of China (grant number 20975089), Department of Science and Technology of Shandong Province of China (grant number 2008GG20005005), One Hundred Person Project of the Chinese Academy of Sciences (grant number 20090462), the National Research Foundation of Korea (grant numbers R11-2009-044-1002-0 and K20904000004-09A050000410), and the KRIBB Research Initiative Program. This work was also partially supported by the Ministry of Knowledge Economy (MKE) and Korea Industrial Technology Foundation (KOTEF) through the Human Resource Training Project for Strategic Technology.

Appendix A. Supplementary data

Supplementary data associated with this article can be found, in the online version, at doi:10.1016/j.bios.2009.11.012.

References

Bagalkot, V., Zhang, L., Levy–Nissenbaum, E., Jon, S., Kantoff, P.W., Langer, R., Farokhzad, O.C., 2007. Nano Lett. 7 (10), 3065–3070.
Becker, R.C., Spencer, F.A., 1998. J. Thromb. Thrombolys. 5 (3), 215–229.
Brody, E.N., Willis, M.C., Smith, J.D., Jayasena, S., Zichi, D., Gold, L., 1999. Mol. Diagn. 4 (4), 381–388.
Bruchez Jr., M., Moronne, M., Gin, P., Weiss, S., Alivisatos, A.P., 1998. Science 281 (5385), 2013–2016.
Chan, W.C.W., Nie, S.M., 1998. Science 281 (5385), 2016–2018.
Chen, L., Choo, J., 2008. Electrophoresis 29 (9), 1815–1828.
Chen, J., Jiang, J., Gao, X., Liu, G., Shen, G., Yu, R., 2008a. Chem. Eur. J 14 (27), 8374–8382.
Chen, L., Lee, S., Lee, M., Lim, C., Choo, J., Park, J.Y., Lee, S., Joo, S.W., Lee, K.H., Choi, Y.W., 2008b. Biosens. Bioelectron. 23 (12), 1878–1882.

Chen, J.W., Liu, X.P., Feng, K.J., Liang, Y., Jiang, J.H., Shen, G.L., Yu, R.Q., 2008c. Biosens. Bioelectron. 24 (1), 66–71.
Chen, X.C., Deng, Y.L., Lin, Y., Pang, D.W., Qing, H., Qu, F., Xie, H.Y., 2008d. Nanotechnology 19 (3), 235105.
Cheng, A.K.H., Su, H., Wang, Y.A., Yu, H.Z., 2009. Anal. Chem. 81 (15), 6130–6139.
Cho, H., Baker, B.R., Wachsmann–Hogiu, S., Pagba, C.V., Laurence, T.A., Lane, S.M., Lee, L.P., Tok, J.B.-H., 2008. Nano Lett. 8 (12), 4386–4390.
Choi, J.H., Chen, K.H., Strano, M.S., 2006. J. Am. Chem. Soc. 128 (49), 15584–15585.
Choi, J.H., Chen, K.H., Han, J.H., Chaffee, A.M., Strano, M.S., 2009. Small 5 (6), 72–675.
Chu, T.C., Shieh, F., Lavery, L.A., Levy, M., Richards-Kortum, R., Korgel, B.A., Ellington, A.D., 2006. Biosens. Bioelectron 21 (10), 1859–1866.
Ellington, A.D., Szostak, J.W., 1990. Nature 346 (6287), 818–822.
Fan, C., Wang, S., Hong, J.W., Bazan, G.C., Plaxco, K.W., Heeger, A.J., 2003. Proc. Natl. Acad. Sci. 100 (11), 6297–6301.
Farokhzad, O.C., Jon, S., Khademhosseini, A., Tran, T–N., LaVan, D.A., Langer, R., 2004. Cancer Res. 64 (21), 7668–7672.
Gersuk, G.M., Carmel, R., Pattengale, P.K., 1989. Blood 74 (7), 2330–2334.
Ghosh, S.K., Pal, T., 2007. Chem. Rev. 107 (11), 4797–4862.
Graham, D., Faulds, K., 2008. Chem. Soc. Rev. 37 (5), 1042–1051.
Hamula, C.L.A., Guthrie, J.W., Zhang, H., Li, X.F., Le, X.C., 2006. Trac-Trends Anal. Chem. 25 (7), 681–691.
Hermann, T., Patel, D.J., 2000. Science 287 (5454), 820–825.
Hu, J., Zheng, P.C., Jiang, J.H., Shen, G.L., Yu, R.Q., Liu, G.K., 2009. Anal. Chem. 81 (1), 87–93.
Huang, C.C., Huang, Y.F., Cao, Z.C., Tan, W.H., Chang, H.T., 2005. Anal. Chem. 77 (17), 5735–5741.
Huang, C.C., Chiang, C.K., Lin, Z.H., Lee, K.H., Chang, H.T., 2008a. Anal. Chem. 80 (5), 1497–1504.
Huang, C.C., Chiu, S.H., Huang, Y.F., Chang, H.T., 2007. Anal. Chem. 79 (13), 4798–4804.
Huang, S.X., Chen, Y., 2008. Nano Lett. 8 (9), 2829–2833.
Huang, Y.F., Chang, H.T., Tan, W.H., 2008b. Anal. Chem. 80 (3), 567–572.
Huang, Y.F., Lin, Y.W., Lin, Z.H., Chang, H.T., 2009. J. Nanopart. Res. 11 (4), 775–783.
Huang, Y.F., Sefah, K., Bamrungsap, S., Chang, H.T., Tan, W.H., 2008c. Langmuir 24 (20), 11860–11865.
Jana, N.R., Ying, J.Y., 2008. Adv. Mater. 20 (3), 430–434.
Javier, D.J., Nitin, N., Levy, M., Ellington, A., Richards–Kortum, R., 2008. Bioconjugate Chem. 19 (6), 1309–1312.
Jung, J., Chen, L., Lee, S., Kim, S., Seong, G.H., Choo, J., Lee, E.K., Oh, C.H., Lee, S., 2007. Anal. Bioanal. Chem. 387 (8), 2609–2615.
Kim, D.K., Kerman, K., Hiep, H.M., Saito, M., Yamamura, S., Takamura, Y., Kwon, Y.S., Tamiya, E., 2008. Anal. Biochem. 379 (1), 1–7.
Kim, S., Chen, L., Lee, S., Seong, G.H., Choo, J., Lee, E.K., Oh, C.H., Lee, S., 2007. Anal. Sci. 23, 401–405.
Lee, J., Jun, H., Kim, J., 2009. Adv. Mater. 21, 1–4.
Lee, J.S., Han, M.S., Mirkin, C.A., 2007a. Angew. Chem. Int. Ed. 46 (22), 4093–4096.
Lee, J.S., Mirkin, C.A., 2008. Anal. Chem. 80 (17), 6805–6808.
Lee, J.S., Ulmann, P.A., Han, M.S., Mirkin, C.A., 2008a. Nano Lett. 8 (2), 529–533.
Lee, J.H., Wang, Z.D., Liu, J., Lu, Y., 2008b. J. Am. Chem. Soc. 130 (43), 14217–14226.
Lee, S., Choi, J., Chen, L., Park, B., Kyong, J.B., Seong, G.H., Choo, J., Lee, Y., Shin, K.H., Lee, E.K., Joo, S.W., Lee, K.H., 2007b. Anal. Chim. Acta 590 (2), 139–144.
Levy, M., Cater, S.F., Ellington, A.D., 2005. ChemBioChem 6 (12), 2161–2166.
Li, H.X., Rothberg, L.J., 2004a. Proc. Natl. Acad. Sci. 101 (39), 14036–14039.
Li, H.X., Rothberg, L.J., 2004b. J. Am. Chem. Soc. 126 (35), 10958–10961.
Liu, C.W., Huang, C.C., Chang, H.T., 2008. Langmuir 24 (15), 8346–8350.
Liu, J., Cao, Z.H., Lu, Y., 2009. Chem. Rev. 109 (5), 1948–1998.
Liu, J., Lee, J.H., Lu, Y., 2007. Anal. Chem. 79 (11), 4120–4125.
Liu, J., Lu, Y., 2003. J. Am. Chem. Soc. 125 (22), 6642–6643.
Liu, J., Lu, Y., 2004. Anal. Chem. 76 (6), 1627–1632.
Liu, J., Lu, Y., 2006. Angew. Chem. Int. Ed. 45 (1), 90–94.
Liu, J., Lu, Y., 2007a. Angew. Chem. Int. Ed. 46 (40), 7587–7590.
Liu, J., Lu, Y., 2007b. Chem. Commun. 46, 4872–4874.
Lou, X., Qian, J., Xiao, Y., Viel, L., Gerdon, A.E., Lagally, E.T., Atzberger, P., Tarasow, T.M., Heeger, A.J., Soh, H.T., 2009. Proc. Natl. Acad. Sci. 106 (9), 2989–2994.
Medley, C.D., Smith, J.E., Tang, Z.W., Wu, Y.R., Bamrungsap, S., Tan, W.T., 2008. Anal. Chem. 80 (4), 1067–1072.
Mirkin, C.A., Letsinger, R.L., Mucic, R.C., Storhoff, J.J., 1996. Nature 382 (6592), 607–609.
Nguyen, T., Hilton, J.P., Lin, Q., 2009. Microfluid Nanofluid 6 (3), 347–362.
Nie, S.M., Emory, S.R., 1997. Science 275 (5303), 1102–1106.
Nimjee, S.M., Rusconi, C.P., Sullenger, B.A., 2005. Annu. Rev. Med. 56, 555–583.
Nitin, N., Javier, D.J., Richards-Kortum, R., 2007. Bioconjugate Chem. 18 (6), 2090–2096.
Park, S.M., Ahn, J.Y., Jo, M., Lee, D.K., Lis, J.T., Craighead, H.G., Kim, S., 2009. Lab. Chip 9 (9), 1206–1212.
Pavlov, V., Xiao, Y., Shlyahovsky, B., Willner, I., 2004. J. Am. Chem. Soc. 126 (38), 11768–11769.
Rex, M., Hernandez, F.E., Campiglia, A.D., 2006. Anal. Chem. 78 (2), 445–451.
Smith, J.E., Medley, C.D., Tang, Z., Shangguan, D.H., Lofton, C., Tan, W.H., 2007. Anal. Chem. 79 (8), 3075–3082.
Song, S.P., Wang, L.H., Li, J., Zhao, J.L., Fan, C.H., 2008. Trac-Trends Anal. Chem. 27 (2), 108–117.
Song, Y., Zhao, C., Ren, J., Qu, X., 2009. Chem. Commun. 15, 1975–1977.
Tallury, P., Kar, S., Bamrungsap, S., Huang, Y.F., Tan, W.H., Santra, S., 2009. Chem. Commun. 17, 2347–2349.
Tanaka, Y., Oda, S., Yamaguchi, H., Kondo, Y., Kojima, C., Ono, A., 2007. J. Am. Chem. Soc. 129 (2), 244–245.
Tuerk, C., Gold, L., 1990. Science 249 (4968), 505–510.
Wang, G., Lim, C., Chen, L., Chon, H., Choo, J., Hong, J., deMello, A.J., 2009a. Anal. Bioanal. Chem. 394 (7), 1827–1832.
Wang, G., Chen, L., 2009b. Chin. Chem. Lett. 20, 1475–1477.
Wang, J., Wang, L.H., Liu, X.F., Liang, Z.Q., Song, S.P., Li, W.X., Li, G., Fan, C., 2007a. Adv. Mater. 19 (22), 3943–3946.
Wang, J., Zhou, H.S., 2008. Anal. Chem. 80 (18), 7174–7178.
Wang, W., Chen, C., Qian, M., Zhao, X.S., 2008a. Anal. Biochem. 373 (2), 213–219.
Wang, Y., Wang, Y., Liu, B., 2008b. Nanotechnology 19 (41), 415605.
Wang, Y., Wei, H., Li, B., Ren, W., Guo, S., Dong, S., Wang, E., 2007b. Chem. Commun. 48, 5220–5222.
Yang, R., Tang, Z., Yan, J., Kang, H., Kim, Y., Zhu, Z., Tan, W., 2008. Anal. Chem. 80 (19), 7408–7413.
Yigit, M.V., Mazumdar, D., Kim, H.K., Lee, J.H., Odintsov, B., Lu, Y., 2007. ChemBioChem 8 (14), 1675–1678.
Yigit, M.V., Mazumdar, D., Lu, Y., 2008. Bioconjugate Chem. 19 (2), 412–417.
Zhang, L., Radovic–Moreno, A.F., Alexis, F., Gu, F.X., Basto, P.A., Bagalkot, V., Jon, S., Langer, R.S., Farokhzad, O.C., 2007. ChemMedChem 2 (9), 1268–1271.
Zhao, W.A., Chiuman, W., Brook, M.A., Li, Y.F., 2007a. ChemBioChem 8 (7), 727–731.
Zhao, W.A., Chiuman, W., Lam, J.C.F., McManus, S.A., Chen, W., Cui, Y.G., Pelton, R., Brook, M.A., Li, Y., 2008. J. Am. Chem. Soc. 130 (11), 3610–3618.